Supporting Information

Mussel Foot Protein Inspired Tough Tissue-Selective Underwater Adhesive Hydrogel

Xianmou Fan[a], Yan Fang[a,*], Weikang Zhou[a], Liyu Yan[a], Yuehua Xu[a], Hu Zhu[b], Haiqing Liu[a,*]

[a]Fujian Provincial Key Laboratory of Polymer Materials, College of Chemistry and Materials Science, Fujian Normal University, Fujian 350007, China

[b]Engineering Research Center of Industrial Biocatalysis, Fujian Province Higher Education Institutes, Fujian 350007, China

[*]Correspondence to: Haiqing Liu (E-mail: haiqingliu@fjnu.edu.cn)

Yan Fang (E-mail:fangyan_YWJ@163.com)

Table of Content

1. Materials and methods

1.1 Materials

Acrylic acid (AA, >99%) and chitin were bought from Shanghai Aladdin Chemical Reagents Co. (China). AA was purified by distillation to remove inhibitor before use. Ammonium persulfate (APS), calcium chloride ($CaCl_2$), magnesium chloride ($MgCl_2$), sodium hydroxide (NaOH), ferric chloride ($FeCl_3$), cellulose microcrystalline, *N,N,N',N'*-tetramethyldiamine (TEMED, 99%), glacial acetic acid, and *N,N'*-methylenebisacrylamide (MBAA) were purchased from Sinopharm (Shanghai, China). All chemicals are analytical grade. Chitosan (CS, M_w = 700 kDa , degree of deacetylation＞90%) was provided by Shanghai Regal Biology Technology Co, Ltd. All these reagents were used as received. Deionized water (pH 6.0) was used in all the experiments. Fresh porcine skins and biological tissues were purchased from a local grocery store, and were rinsed with water before use. Natural seawater was taken from a local ocean.

Mouse fibroblast L929 cells were provided by iCell Bioscience Inc (Shanghai, China). The cells were cultured in a medium (Biosharp) with high glucose containing 10% horse serum (Shanghai Yuanye Bio-Technology Co., Ltd) at 37 °C in 5% CO_2 humidified atmosphere.

Chinese lacquer was bought from Institute of Lacquer, Xi'an, China. From it urushiol was extracted with ethanol[1]. Briefly, 1 kg of Chinese lacquer sap was dissolved in 2 L of ethanol under mechanically stirring for 24 h at room temperature, followed by filtration to collect filtrate. After ethanol was removed by vacuum-rotary evaporation at 60 °C, urushiol was obtained. UCAT was isolated and purified following a reported column

chromatography method[2].

1.2 Fabrication of PAA-CS polyelectrolyte hydrogel. CS (0.1, 0.2, 0.3, 0.4, and 0.5 g, which is 1.0, 2.0, 3.0, 4.0, 5.0 % of AA) was dissolved in 30 mL of 2 vol% aq. acetic acid solution under stirring to obtain a homogeneous solution. It was then mixed with AA (10.0 g), MBAA (0.025 g), APS (0.05 g) under stirring for 30 min at 25 °C. Into it TEMED (40 μL) was then added under stirring for 15 min. Subsequently the mixed solution was added into molds and polymerized at 70 °C for 24 h. All percent is weight percent unless otherwise specified.

1.3 Fabrication of P(AA-co-UCAT$_x$)-CS$_y$ polyelectrolyte hydrogels. The formula of these hydrogels are shown in Table S1. Typically, a CS solution was prepared by dissolving CS powder in 2 vol% aq. acetic acid solution at 25 °C (solution A). UCAT was mixed with AA, MBAA, and APS under magnetically stirring for 30 min under ambient conditions (solution B). Then solution A and B were mixed in an ice bath under stirring for 5 min. A free-standing P(AA-co-UCAT$_x$)-CS$_y$ hydrogel was quickly formed at room temperature upon the ice bath was removed, where x and y are the mass ratio of UCAT/AA and CS/AA, respectively. The pH of the hydrogel was 4-5. The water content in the hydrogels was in a range of 72.3-74.3%. A dry hydrogel was prepared by freeze-drying a hydrogel fully cleaned with water (3 times a day for 5 days) in a freeze dryer (ALPHA1-2/LD-Plus).

1.4 Preparation of chitin, cellulose, and chitosan film

Chitin, cellulose, and chitosan films were fabricated via the solution-casting method. Briefly, 4 g of chitin was dissolved in 100 g of 11 wt% NaOH and 4 wt% urea

aqueous solution via a freeze-thaw process to obtain a transparent chitin solution. Then, the chitin solution was cast on a glass plate with a 0.5 mm thickness layer and then immersed into an ethanol coagulant for 2 h at 5 ^{o}C for regeneration. After completely cleaned with distilled water, a chitin membrane was obtained. A similar process was used for the preparation of cellulose membrane, except for the solvent. Cellulose was dissolved in 7.5 wt% NaOH and 11 wt% urea aqueous solution. As for chitosan membrane, 4 g of chitosan was dissolved in 60 ml of 2 wt% acetic acid solution under stirring to obtain a homogeneous chitosan solution. The resultant chitosan solution was cast on a glass plate with a 0.5 mm thickness layer and then the chitosan membrane was cleaned with 1:3 water–ethanol solution.

1.5 Formulation of simulated body fluid (SBF)

NaCl (8.035 g), $NaHCO_3$ (0.355 g), KCl (0.225 g), $K_2HPO_4 \cdot 3H_2O$ (0.231 g), $MgCl_2 \cdot 6H_2O$ (0.311 g), 1.0 M HCl (39 ml), $CaCl_2$ (0.292 g), Na_2SO_4 (0.072 g), and tris(hydroxymethyl)methyl aminomethane (6.118 g) were dissolved in water (1000 mL) to prepare SBF. The ion concentration in the SBF was shown in Table S2.

2. Characterization and testing methods

2.1 Gelation time

The gelation time of the hydrogel was characterized by the vial inverting method. Briefly, the reaction mixture solution (4 mL) was poured into a vial and then incubated in a 25 ^{o}C water bath. When the bottle was inverted vertically, no visible flow within 60 s was considered as a standard for gel formation. All experiments were performed in

triplicate.

2.2 Mechanical property

The tensile and compression properties of the hydrogels were evaluated on an electrical universal testing machine equipped with a 500 N load cell (Lloyd, LR5k) at 25 ^{o}C according to ASTM-638-V. A cylindrical gel with height of 12 mm and diameter of 10 mm was used for the compression test. It was compressed to 90% strain at a speed of 50 mm/min. A dumbbell hydrogel (25 (l) × 4(w) × 4(t) mm^3) was used for the tensile and fracture toughness tests. The crosshead rate for the tensile test was 100 mm/min. The fracture toughness was calculated by Equation (1)[3]:

$$Fracture\ toughness = \frac{U(\varepsilon_c)}{a_0 b_0} \quad (1)$$

where a_0 and b_0 are the width and thickness of the hydrogel, respectively; $U(\varepsilon_c)$ is the area under the force-strain curve (F-ε) from ε = 0 to critical strain (n = 5).

2.3 Tearing test

Hydrogels (40 (l) × 20 (w) × 4 (t) mm^3) was cut into a trousers shape with an initial notch of 5 mm. One arm of the hydrogel was clamped and the other was fixed. It was pulled upward at a rate of 50 mm/min. The tearing energy is defined as the work required to tear a unit area, and is calculated according to Equation (2):

$$Tearing\ energy = \frac{2F_{ave}}{w} \quad (2)$$

where F_{ave} is the average force of peak value during steady-state tear and w is the width of the hydrogel (n = 5).

2.4 Lap shear adhesion strength of hydrogel to substrates

The adhesion strength of hydrogel to fresh wet porcine skin was conducted by sandwiching a hydrogel with size of 25 (w) × 20 (l) mm^2 between two porcine skins (Fig. S1a), followed by statically placing at ambient conditions for 30 min before tensile tests. The sample was pulled to failure by the universal testing machine with a cross-head speed of 50 mm/min at 25 °C. The adhesion strength of hydrogel to tinplate and glass was measured by the same procedure. To test the recyclability of the adhesive hydrogel to porcine skin, aq. NaOH solution (pH 8.0) was sprayed onto the hydrogel/skin interface. Five min later, the hydrogel was peeled off. Then it was rinsed to neutrality with distilled water. The free water on the hydrogel surface was sucked with filter paper before re-applied onto porcine skin for re-evaluation of adhesion strength.

2.5 Interfacial toughness of hydrogel to porcine skin

The interfacial toughness of hydrogel was investigated via the 90-degree peeling test by following the standard ASTM D 2861[4]. A hydrogel with size of 80 (l) × 10 (w) × 4 (t) mm^3 was adhered to a porcine skin (Fig. S1b), followed by storing for 30 min at ambient conditions. The crosshead speed was 50 mm/min. The interfacial toughness is calculated by Equation (3)[5]:

$$Interfacial\ toughness = \frac{F_{ave}}{w} \qquad (3)$$

where F_{ave} is the average force at the plateau in the steady-state (or plateau) of the curve. If a steady state is not reached, the force at the breaking point is used; w is the width of the

hydrogel sheet (n = 5).

2.6 Adhesion energy of hydrogel to porcine skin

The adhesion energy was conducted according to a reported method[6]. The setup was shown in Fig. S1c. A hydrogel (20 (*l*) × 15 (*w*) × 3 (*t*) mm^3) was sandwiched between two porcine skins with size of 80 (*l*) × 15 (*w*) × 5 (*t*) mm^3, followed by storing for 30 min at ambient conditions. The loading rate was 100 mm/min. The adhesion energy was determined as two times the plateau force value at the steady-state per width (Adhesion energy = $2F/w$). To test the effect of storing time on adhesion, the hydrogel was stored in a sealed aluminum foil bag at room temperature. Then the adhesion energy to porcine skins was measured every 6 days for successive 30 days. As for measuring the adhesion energy of a hydrogel to blood-stained biological tissue, fresh porcine blood was applied onto the surface of each porcine skin, then the hydrogel was immediately applied. After 30 min, the adhesion energy was measured according to the same procedure (n = 5).

2.7 Bursting pressure of hydrogel on porcine intestine

Bursting pressure test was performed following a protocol reported previously[7]. A porcine small intestine was used in this test. Each end of a three-way tube was connected to the porcine small intestine, a nitrogen tank, and a pressure gauge, respectively. A hole of 3 mm in diameter was made on the intestine. A hydrogel with size of 25 (*l*) × 20 (*w*) × 2 (*t*) mm^3 was adhered onto the intestine to cover the hole, and was kept for 5 min. Then the intestine was slowly inflated with nitrogen gas. The pressure increased with inflation, then dropped when the hole was burst. The highest-pressure value was recorded as the

bursting pressure (n = 3).

2.8 Torsion on wet tissue

A hydrogel was pressed on an underwater fresh porcine skin until it firmly attached to the skin. Then stress of torsion, twist, and fold was applied to the skin to test the adherence flexibility.

2.9 Underwater adhesion test

In water with pH of 6.0, 8.0, 9.0 or 11.0, the hydrogel was sandwiched between two porcine skins with a bonding area of 20 × 15 mm^2, and left in water for additional 2 min. Then, it was taken out and placed in air for 30 min before tensile test according to the setup shown in Fig. S1c. For the effect of water-soaking time on adhesion, the skin/hydrogel/skin sandwich was kept in water (pH 6.0) for 2, 4, 6 and 8 h, while the other procedure was kept same.

2.10 Cytotoxicity Assays

The cytotoxicity of the extract of hydrogel was evaluated. In detail, 0.1 g of P(AA-co-PUCAT)-CS hydrogel was placed in a sterile Petri dish. Into it, 1 mL of absolute ethanol was added, followed by sterilization under UV light for 1 h. Excess alcohol in the hydrogel was removed by evaporation, then the hydrogels were washed with sterile PBS (Procell). The extract was made by incubating the sterilized hydrogel in 1 mL of complete culture medium for 24 h at 37 °C.

The cytotoxicity of hydrogel was evaluated by incubating the extract of hydrogel with L929 mouse fibroblast cells according to the procedure reported by Zhou et al[8]. 200 μL of

L929 cell suspension was seeded in 96-well plate at a concentration of 4×10^3 cells/well and allowed to adhere for 48 h at 37 °C in a humidified atmosphere containing 5% CO_2. The culture media was then removed and 0.2, 1.0, 5.0, 20.0 and 50 mg/ml of the extract medium were added to each well. After 48 h, the medium was removed and 100 μL of MTT (Beijing Solarbio Science□Technology Co., Ltd. 0.5 mg/mL in PBS) solution was added to each well, followed by incubation at 37 °C (5% CO_2) for 4 h. Finally, all medium was removed and 100 μL/well DMSO was added, followed by shaking for 15 min. The absorbance of each well was measured at 570 nm with pure DMSO as a control using a microtiter plate reader. The relative cell viability is calculated by Equation (4):

$$Relative\ cell\ viability(\%) = \frac{Abs_{sample}}{Abs_{control}} \times 100\% \quad (4)$$

where Abs_{sample} and Abs_{control} represent the absorbance of the sample and control, respectively (n = 3).

After incubation for 48 h at 37 ºC in 5% CO_2, the live/dead cells were assessed using a live fluorescent staining assay kit (DiO, Beyotime Biotechnology, Shanghai, China) following the manufacturer's protocol. Briefly, the cells were cultured in 24-well culture plates with extract, and at the end of the incubation period, the medium was removed and 100 μL of the staining reagent was added after the cells were gently washed with PBS. The staining reagent was removed after incubation for 30 min at 37 °C in darkness. 100 μL of normal culture medium was added into the well after the cells were gently washed with PBS. The cells were then observed under a confocal laser scanning microscope (FV1200,

Olympus).

2.11 Fourier transform infrared spectroscopy and scanning electron microscopy

Fourier transform infrared spectroscopy (FTIR) of samples in KBr form was performed at room temperature on a Nicolet FTIR spectrometer (Thermo Scientific, USA). All spectra were obtained with 32 scans and a resolution of 2 cm^{-1} in the range of 4000−400 cm^{-1}. The microstructure of hydrogels was observed on JEOL-7500LV field emission scanning electron microscopy (SEM) at an accelerating voltage of 3 kV. The samples were prepared by freeze-drying and then cryogenically fractured in liquid nitrogen. Before SEM observation, the fractured surface was sputter-coated with a thin layer of gold at 30 mA for 150 s.

2.12 Swelling test of the P(AA-co-UCAT)-CS hydrogel

A dry hydrogel (m_0) was immersed in 50 mL of PBS at 37 °C for 24 h. The swollen hydrogel was taken out and weighed (m_e) after excess water on the surface was sucked with filter papers. Triplicates were run for each hydrogel. The swelling ratio was calculated according to Equation (5).

$$Swelling\ ratio = \frac{m_e - m_0}{m_0} \times 100\ \% \qquad (5)$$

2.13 Statistical analysis

Data were presented as mean ± standard deviation. Statistically significant differences ($p<0.05$) and extraordinary significant difference ($p<0.01$) between experimental groups

were determined by a Student's t-test and ANOVA with spss 19.0.

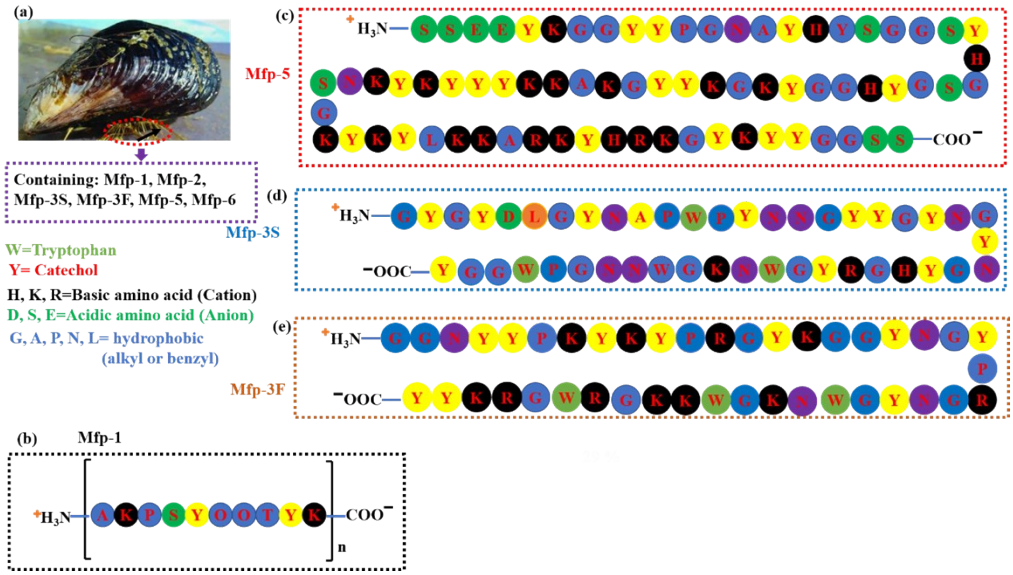

Scheme S1 (a) A mussel adheres to a wet rock through byssal plaques shown in the red dotted circle. Mussel foot proteins (Mfps) Mfp-1, Mfp-2, Mfp-3S, Mfp-3F, Mfp-5, and Mfp-6 coexist in the plaque front. Amino acid sequence of (b) Mfp-1, (c) Mfp-5, (d) Mfp-3S, and (e) Mfp-3F[9-11].

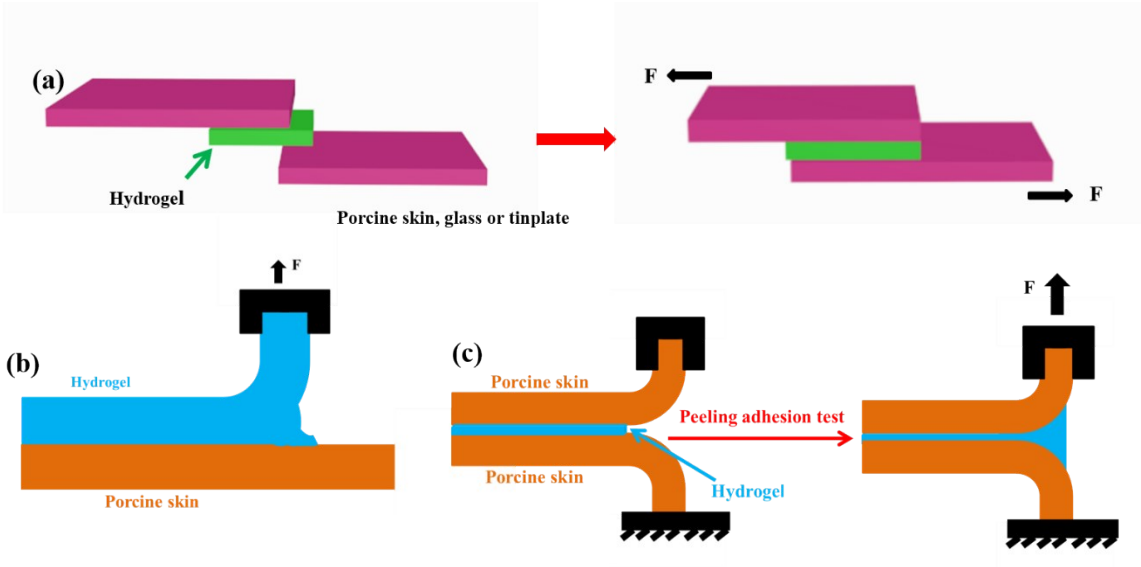

Fig. S1 (a) Schematic setup for the lap-shear adhesion of hydrogel to porcine skin, glass or tinplate. (b) Schematic diagram of the peeling test. (c) Adhesion energy measured by the 180-dergee peeling test.

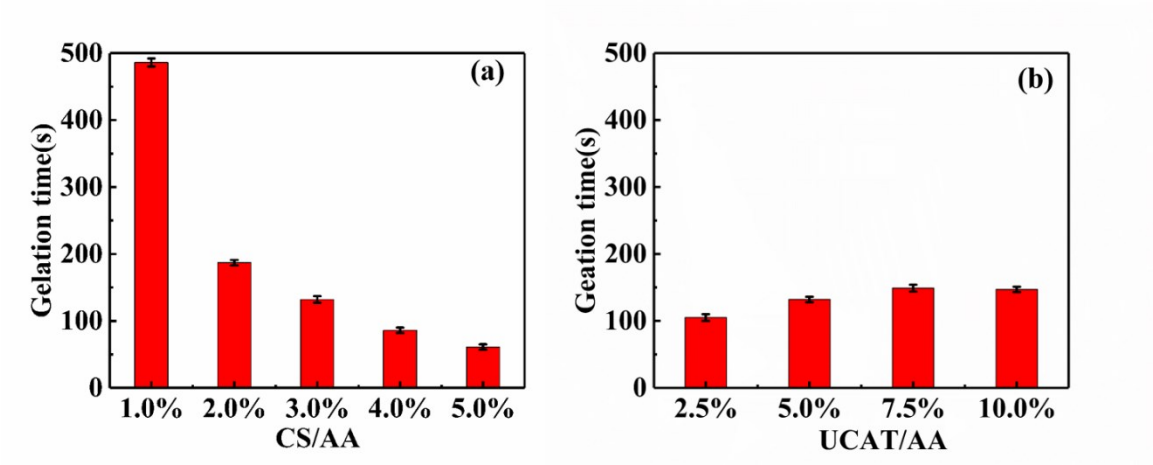

Fig. S2 Hydrogel gelation time as a function of (a) CS and (b) UCAT content in the reaction formula shown in Table S1. P(AA-co-$UCAT_5$)-CS_1 hydrogel had the longest gelation time of about 486 s, whereas the gelation time of P(AA-co-$UCAT_5$)-CS_5 hydrogel was much shorter (ca. 60 s).

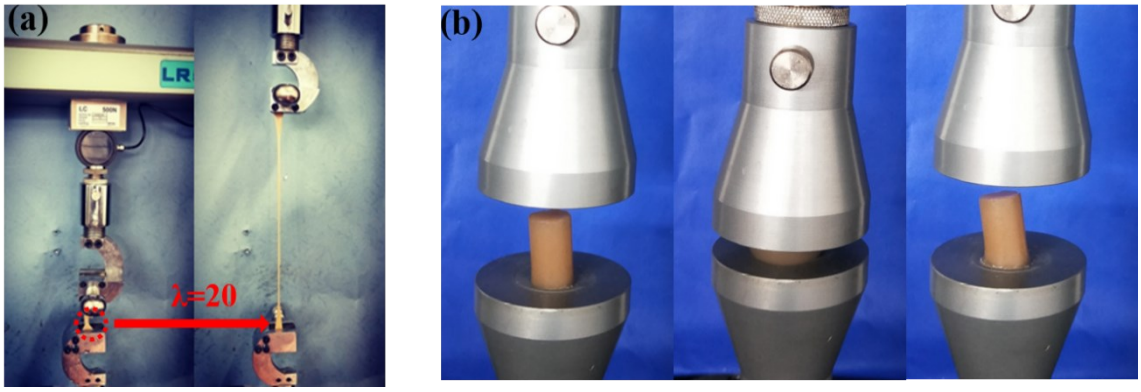

Fig. S3 (a) Digital photos showed the P(AA-co-$UCAT_5$)-CS_3 hydrogel was stretched to 20 times its initial length. (b) P(AA-co-$UCAT_5$)-CS_3 hydrogel recovered to its original shape after it was compressed to a strain of 90%.

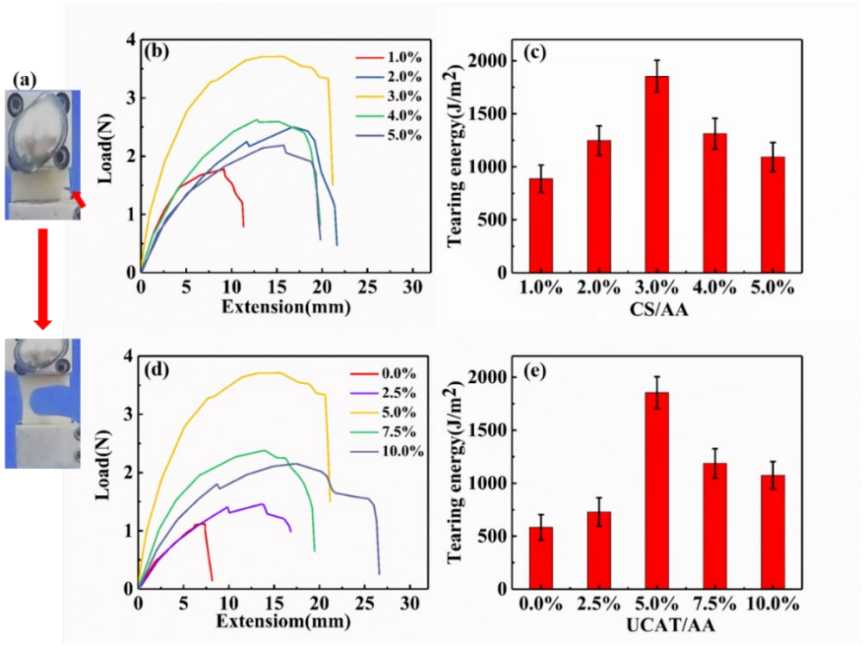

Fig. S4 (a) Crack resistance of a notched P(AA-co-UCAT$_5$)-CS$_3$ hydrogel. Typical tearing force-extension curves of P(AA-co-UCAT)-CS hydrogels as a function of (b) CS/AA and (d) UCAT/AA. Tearing energy of P(AA-co-UCAT)-CS hydrogels as a function of (c) CS/AA and (e) UCAT/AA.

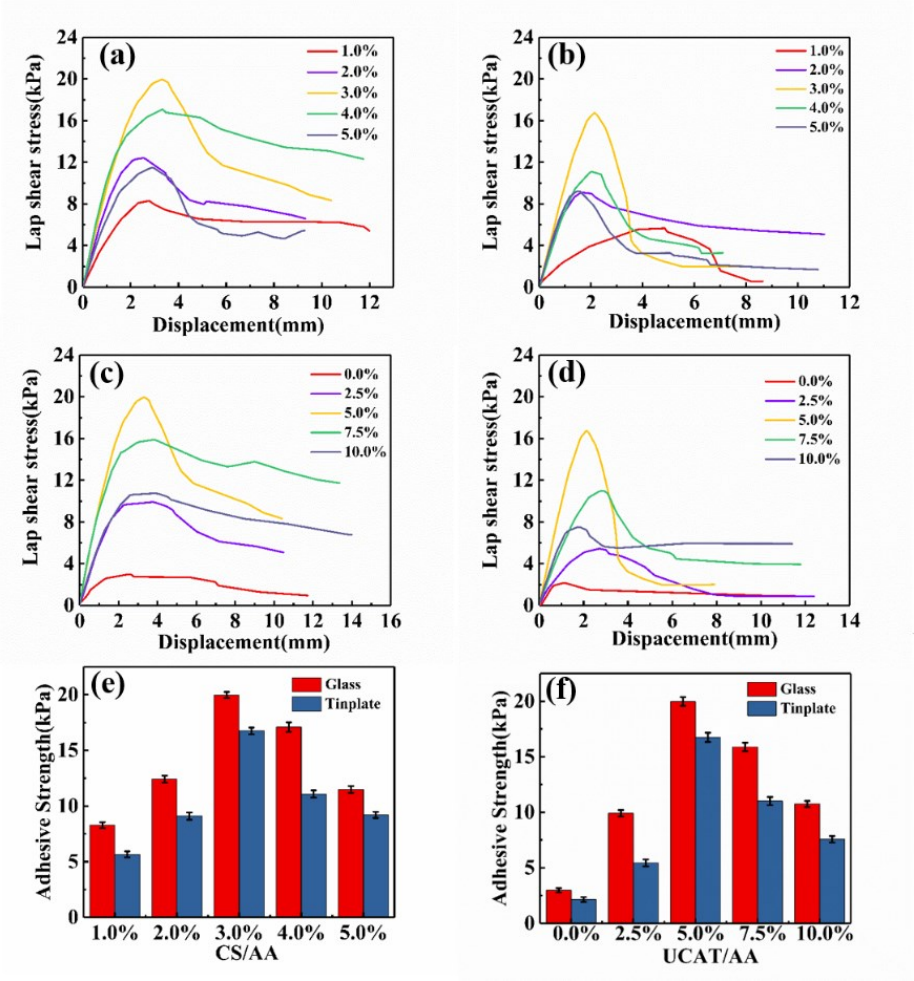

Fig. S5 Typical lap shear stress-displacement curves of P(AA-co-$UCAT_5$)-CS_3 hydrogel to glass as a function of (a) CS/AA and (c) UCAT/AA, and to tinplate as a function of (b) CS/AA and (d) UCAT/AA. Adhesion strength of the hydrogel to (e) glass and (f) tinplate.

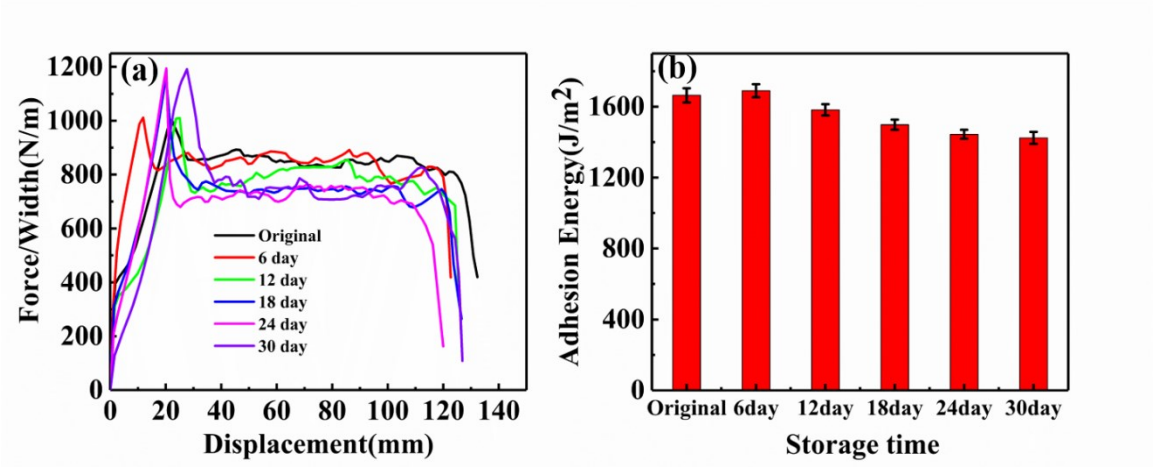

Fig. S6 180-degree peeling test results for P(AA-co-UCAT$_5$)-CS$_3$ hydrogel that was stored in a sealed aluminum foil bag at room temperature for 6, 12, 18, 24 and 30 days. (a) Typical force-displacement curves of peeling hydrogels off from porcine skin after stored for different time. (b) Adhesion energy of hydrogel to porcine skin as a function of storing time.

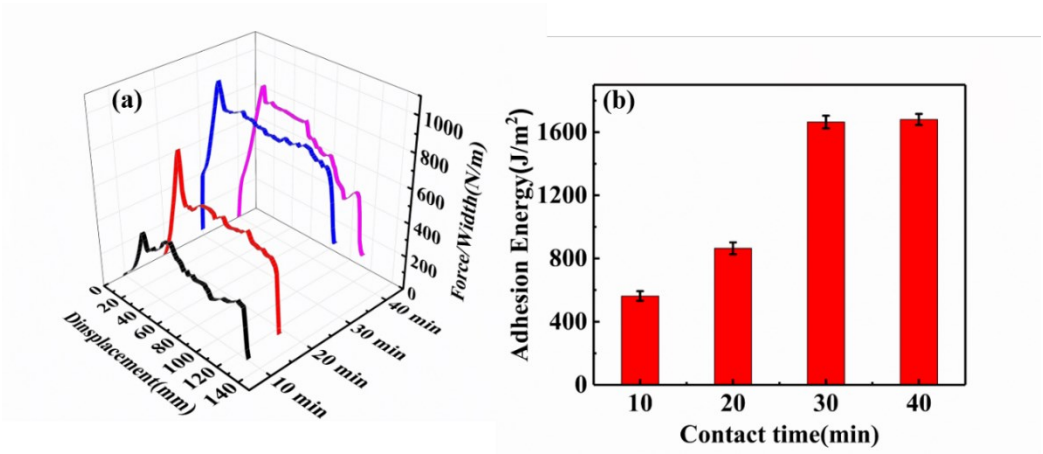

Fig. S7 Effect of contact time between hydrogel and porcine skin on adhesion energy. (a) Typical force-displacement curves of peeling off a hydrogel from porcine skin. (b) Adhesion energy of hydrogel to porcine skin as a function of contact time.

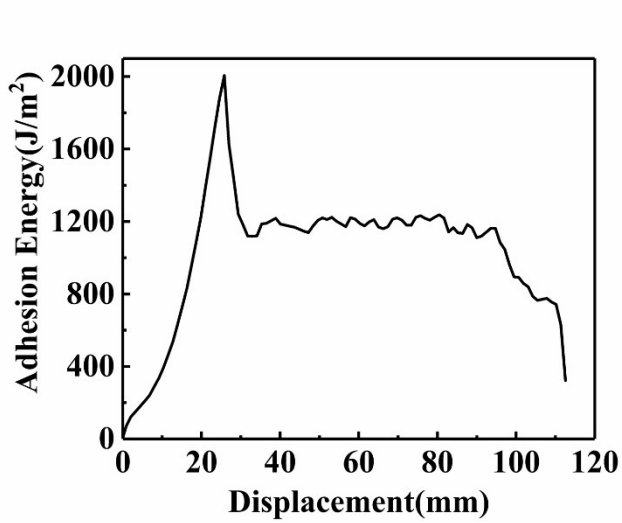

Fig. S8 Adhesion energy of P(AA-co-$UCAT_5$)-CS_3 hydrogel to seawater wetted porcine skin.

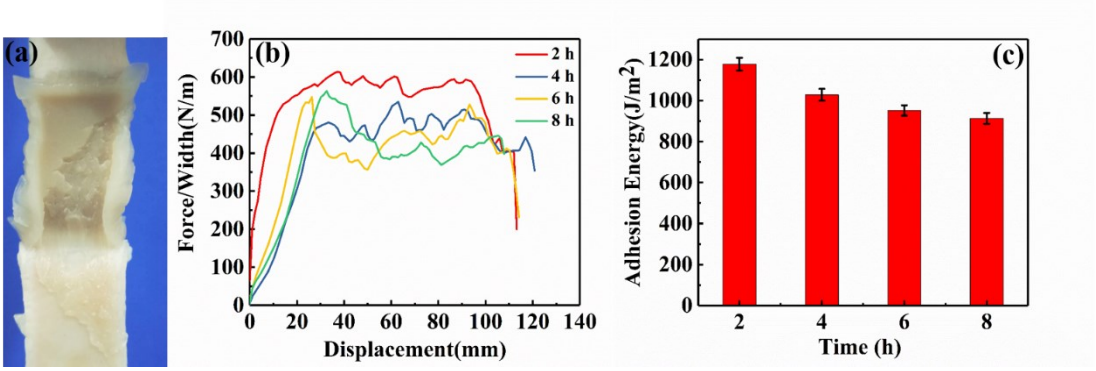

Fig. S9 Effect of water-soaking time on adhesion energy of P(AA-co-$UCAT_5$)-CS_3 hydrogel to porcine skin. (a) A typical photo for adhesion energy test of two porcine skins bonded with a P(AA-co-$UCAT_5$)-CS_3 hydrogel after soaked in water for 6 h. (b) Typical adhesion force-displacement curves for bonded porcine skin soaked in water for certain time interval. (c) Adhesion energy as a function of water-soaking time.

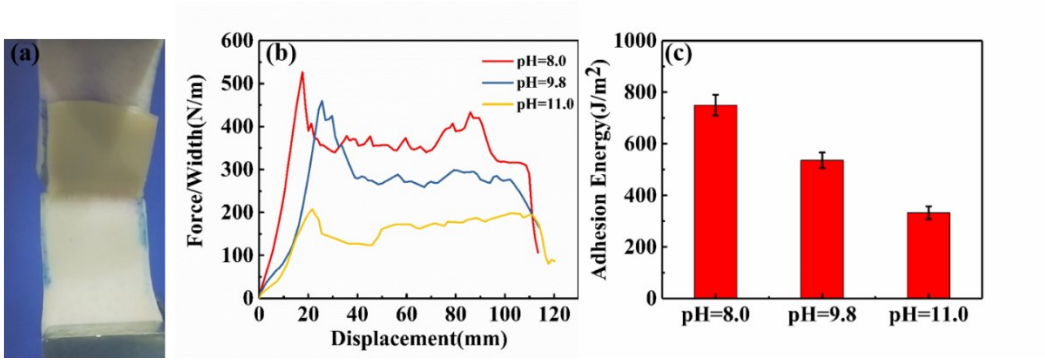

Fig. S10 Effect of pH on adhesion energy of P(AA-co-UCAT$_5$)-CS$_3$ hydrogel to porcine skin. (a) A digital photo of the peeling test of porcine skins bonded with P(AA-co-UCAT$_5$)-CS$_3$ hydrogel in the presence of pH 8.0 solution. (b) Typical force-displacement curves for the peeling test of porcine skins bonded with P(AA-co-UCAT$_5$)-CS$_3$ in the presence of pH solutions. (c) Effect of pH value on adhesion energy of P(AA-co-UCAT$_5$)-CS$_3$ to porcine skin.

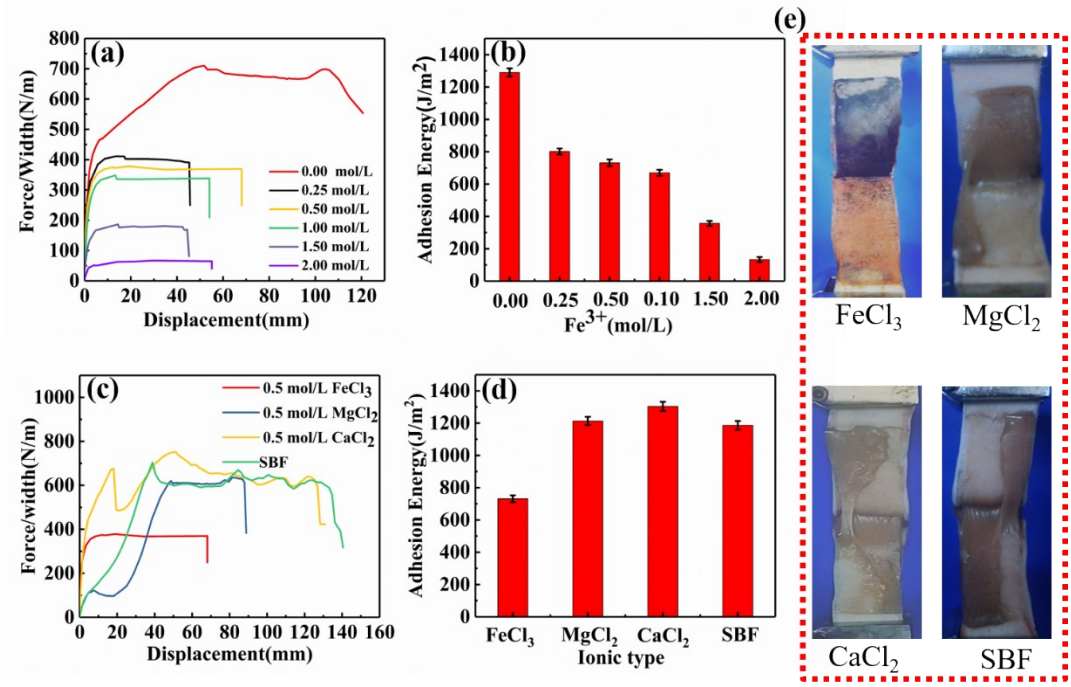

Fig. S11 Effect of Fe^{3+}, Mg^{2+}, and Ca^{2+} on adhesion energy of P(AA-co-UCAT$_5$)-CS$_3$ hydrogel to porcine skin. (a) Typical force-displacement curves for the peeling test of

porcine skins bonded with P(AA-co-$UCAT_5$)-CS_3 in the presence of $FeCl_3$ solution with different concentrations. (b) Effect of $FeCl_3$ concentration on adhesion energy of P(AA-co-$UCAT_5$)-CS_3. (c) Typical force-displacement curves for the peeling test of porcine skins bonded with P(AA-co-$UCAT_5$)-CS_3 in the presence of 0.5 mol/L $FeCl_3$, $MgCl_2$, and $CaCl_2$ solution. (c) Effect of 0.5 mol/L $FeCl_3$, $MgCl_2$, and $CaCl_2$ solution on adhesion energy of P(AA-co-$UCAT_5$)-CS_3. (e) Digital photos of the peeling test of porcine skins bonded with P(AA-co-$UCAT_5$)-CS_3 hydrogel in the presence of $FeCl_3$, $MgCl_2$, and $CaCl_2$ solution (conc. 0.5 mol/L).

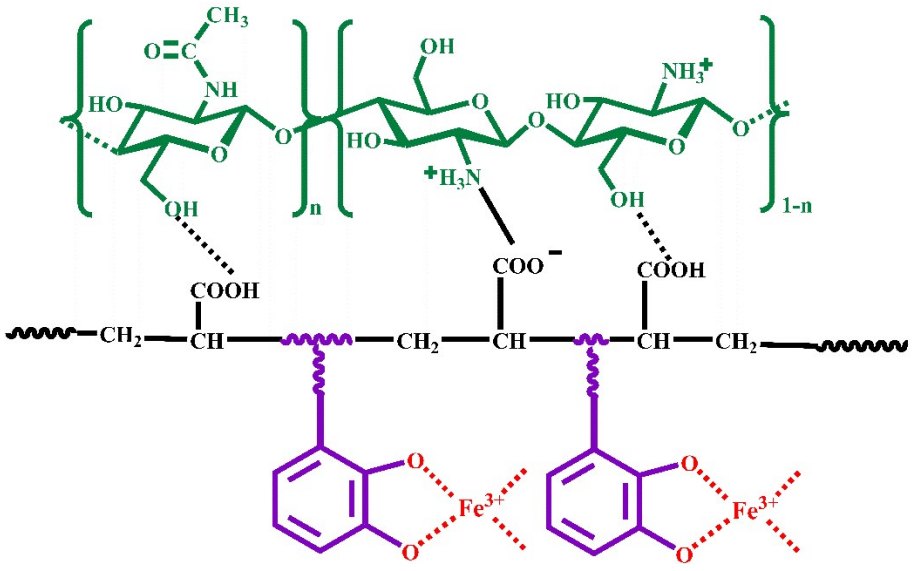

Fig. S12 Inactivation of catechol by interaction between Fe^{3+} and catechol units in P(AA-co-PUCAT)-CS hydrogel.

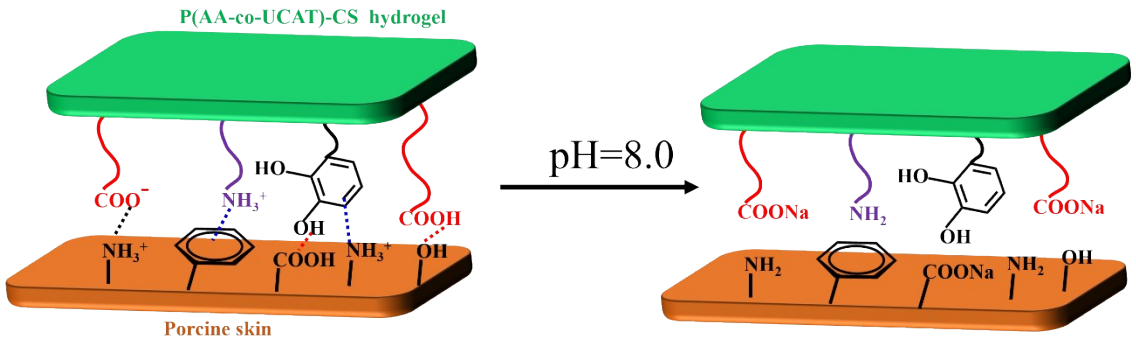

Fig. S13 Interfacial debonding mechanism in the presence of aq. basic solution (pH 8.0).

The structure and physical properties of the dry P(AA-co-UCAT$_5$)-CS$_3$ hydrogel was validated by SEM, FT-IR, and swelling ratio (Fig. S14). SEM revealed that the lyophilized P(AA-co-UCAT$_5$)-CS$_3$ and PAA-CS hydrogel had a porous structure (Fig. S14a and b). FTIR results of the P(AA-co-UCAT$_5$)-CS$_3$ and PAA-CS$_3$ hydrogels (Fig. S14c) showed very similar curve patterns. The peaks at 1713 cm^{-1} and 2930 cm^{-1} respectively correspond to the stretching vibration of C=O of PAA and C–H of alkyl chain of PUCAT.

After equilibrium swelling, the hydrogel well maintained its original square shape, and the surface area of the hydrogel increased by a factor of four, demonstrating that our hydrogel was an isotropic hydrogel (Fig. S14d). The content of UCAT in the fixed hydrogel was 5.0%. When the CS content increased from 1.0% to 5.0%, its saturated swelling ratio significantly reduced from 17.20 g/g to 8.51 g/g (Fig. S14e). This may be because CS and PAA form more physical cross-linking points through electrostatic interaction, which limits the stretching of the PAA chain, thereby reducing the degree of swelling. The CS content in the fixed hydrogel was 3%. As the UCAT dosage increased from 2.5% to 10.0%,

the saturated swelling ratio of the hydrogel increased from 8.35 g/g to 14.30 g/g and then decreased to 8.82 g/g (Fig. S14f). UCAT is a catechol derivative having a long chain hydrophobic alkyl group in its side chain. When it was contained in the hydrogel, its hydrophobic alkyl chain was easily aggregated by hydrophobic interaction, and the π-π interaction tended to aggregate the urushiol, resulting in an increase in the crosslinking point and limiting swelling.

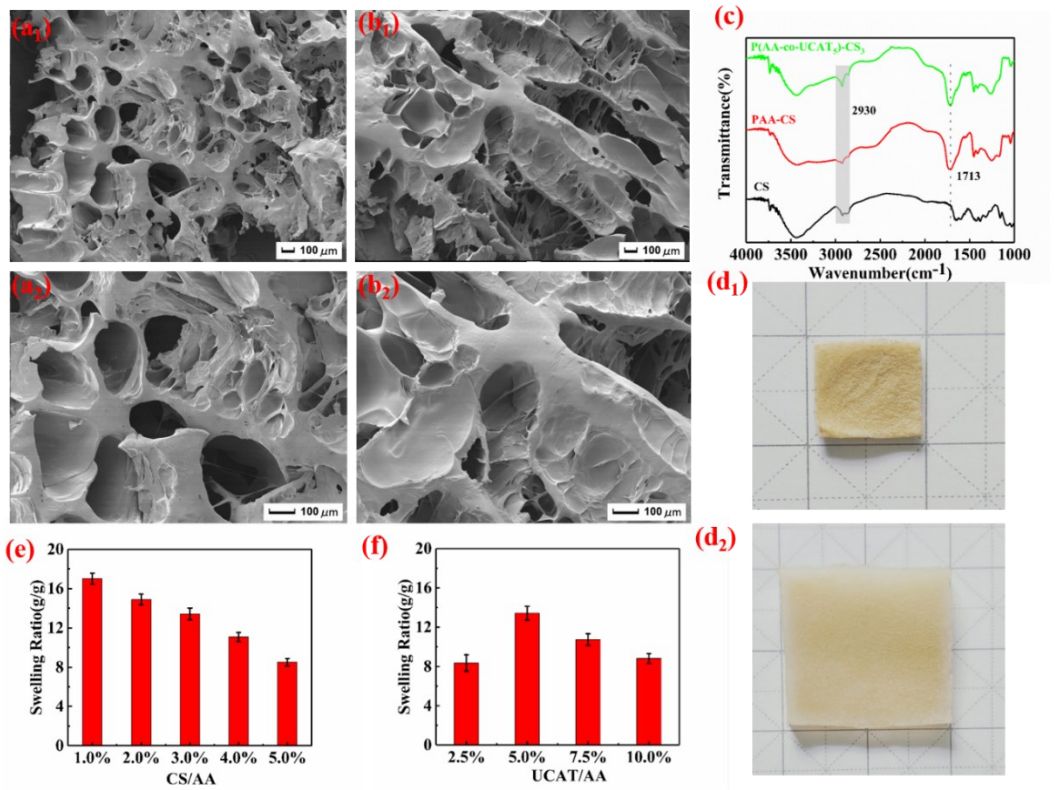

Fig. S13 SEM images of fractured (a) P(AA-co-UCAT$_5$)-CS$_3$ and (b) PAA-CS$_3$ hydrogel. (c) FITR spectra of dry CS, PAA-CS$_3$, and P(AA-co-UCAT$_5$)-CS$_3$ hydrogels. (d) Photos of P(AA-co-UCAT$_5$)-CS$_3$ hydrogel before and after equilibrium swollen in PBS for 24 h at 37 ℃. Swelling ratio of P(AA-co-UCAT)-CS hydrogel as a function of (e) CS/AA and

(f) UCAT/AA, after soaked in PBS for 24 h at 37 ℃ (n=3).

Table S1. Composition of the prepared hydrogels

Hydrogels	AA (g)	CS/AA (%)	UCAT/AA (%)	MBAA/AA (%)	APS/AA (%)	H_2O (g)	Water content (%)
P(AA-co-UCAT$_{2.5}$)-CS$_1$		1.0					74.3
P(AA-co-UCAT$_{2.5}$)-CS$_2$		2.0					74.2
P(AA-co-UCAT$_{2.5}$)-CS$_3$	10.0	3.0	2.5	0.25	0.5	30	74.0
P(AA-co-UCAT$_{2.5}$)-CS$_4$		4.0					73.8
P(AA-co-UCAT$_{2.5}$)-CS$_5$		5.0					73.6
P(AA-co-UCAT$_5$)-CS$_1$		1.0					73.9
P(AA-co-UCAT$_5$)-CS$_2$		2.0					73.7
P(AA-co-UCAT$_5$)-CS$_3$	10.0	3.0	5.0	0.25	0.5	30	73.5
P(AA-co-UCAT$_5$)-CS$_4$		4.0					73.3
P(AA-co-UCAT$_5$)-CS$_5$		5.0					73.2
P(AA-co-UCAT$_{7.5}$)-CS$_1$		1.0					73.4
P(AA-co-UCAT$_{7.5}$)-CS$_2$		2.0					73.3
P(AA-co-UCAT$_{7.5}$)-CS$_3$	10.0	3.0	7.5	0.25	0.5	30	73.1
P(AA-co-UCAT$_{7.5}$)-CS$_4$		4.0					72.9
P(AA-co-UCAT$_{7.5}$)-CS$_5$		5.0					72.7
P(AA-co-UCAT$_{10}$)-CS$_1$		1.0					72.9
P(AA-co-UCAT$_{10}$)-CS$_2$		2.0					72.8
P(AA-co-UCAT$_{10}$)-CS$_3$	10.0	3.0	10.0	0.25	0.5	30	72.6
P(AA-co-UCAT$_{10}$)-CS$_4$		4.0					72.5
P(AA-co-UCAT$_{10}$)-CS$_5$		5.0					72.3

Note: All percent are weight percent unless otherwise specified.

Table S2 Ion concentration (mM) in the SBF formulation

Ion	Na^+	K^+	Mg^{2+}	Ca^{2+}	Cl^-	HCO_3^-	HPO_4^{2-}	SO_4^{2-}
Concentration	142.0	5.0	1.5	2.5	147.8	4.2	1.0	0.5

References:

1. X. Fan, W. Zhou, Y. Chen, L. Yan, Y. Fang and H. Liu, *ACS Appl. Mater. Interfaces*, 2020, **12**, 32031–32040.
2. Z. Qi, C. Wang and J. Jiang, *Molecules*, 2018, **23**, 1074.
3. F. Wang and R. A. Weiss, *Macromolecules*, 2018, **51**, 7386-7395.
4. H. Yuk, T. Zhang, S. Lin, G. A. Parada and X. Zhao, *Nat. Mater.*, 2016, **15**, 190-196.
5. H. Chen, Y. Liu, B. Ren, Y. Zhang, J. Ma, L. Xu, Q. Chen and J. Zheng, *Adv. Funct. Mater.*, 2017, **27**, 1703086.
6. J. Li, A. Celiz, J. Yang, Q. Yang, I. Wamala, W. Whyte, B. Seo, N. Vasilyev, J. Vlassak and Z. Suo, *Science*, 2017, **357**, 378-381.
7. Y. Bu, L. Zhang, J. Liu, L. Zhang, T. Li, H. Shen, X. Wang, F. Yang, P. Tang and D. Wu, *ACS Appl. Mater. Interfaces*, 2016, **8**, 12674-12683.
8. D. Zhou, S. Li, M. Pei, H. Yang, S. Gu, Y. Tao, D. Ye, Y. Zhou, W. Xu and P. Xiao, *ACS Appl. Mater. Interfaces*, 2020, **12**, 18225-18234.
9. B. K. Ahn, S. Das, R. Linstadt, Y. Kaufman, N. R. Martinez-Rodriguez, R. Mirshafian, E. Kesselman, Y. Talmon, B. H. Lipshutz, J. N. Israelachvili and J. H. Waite, *Nat. Commun.*, 2015, **6**, 8663.
10. S. Seo, S. Das, P. J. Zalicki, R. Mirshafian, C. D. Eisenbach, J. N. Israelachvili, J. H. Waite and B. K. Ahn, *J. Am. Chem. Soc.*, 2015, **137**, 9214.
11. W. Wei, J. Yu, C. Broomell, J. N. Israelachvili and J. H. Waite, *J. Am. Chem. Soc.*, 2013, **135**, 377.